

THE COUPLED STRUCTURAL-ACOUSTIC ANALYSIS OF SPACECRAFT SOLAR ARRAYS BASED ON THE FEM-BEM METHOD

Yuanjie Zou

Institute of Spacecraft System Engineering, CAST, Beijing, 100094

email: yuanjiez@qq.com

Qiang Gao

Beijing Institute of Electronic System Engineering, Beijing, 100854

Weihong Zhu, Zengyao Han

Institute of Spacecraft System Engineering, CAST, Beijing, 100094

The analysis of the vibration responses for stacked solar arrays exposed to a reverberant acoustic excitation has been a heated research subject in the field of spacecraft structural dynamics for years, since the thin and light solar arrays are very sensitive to the acoustic field which could bring about severe damage to the structure. This type of analysis is very difficult, because the peculiar random acoustic excitation is hard to simulate accurately, and the solar array panels are strongly coupled with the narrow cavities between the panels. The FEM (Finite Element Method)-BEM (Boundary Element Method) method provides an effective way to analyze this coupling problem in the low frequency (eg, below 100Hz). Usually, the plane waves are applied to simulate the reverberant acoustic field. This paper presents a method to model an acoustic diffuse field by combining uncorrelated plane waves linearly and proves its veracity theoretically. The parameters for each plane wave are also obtained through derivation in the paper. After that, the vibro-acoustic problem for spacecraft solar arrays is simulated using FEM-BEM method and the results are validated by the test data, which shows that the method is theoretically correct and could be used to analyze the vibro-acoustic response of spacecraft. Besides, it is shown that there is a notable SPL (Sound Pressure Level) increase in the narrow air gaps between panels if the excitation frequency becomes closer to the narrow cavity resonance modes.

Keywords: spacecraft, vibration, boundary element method

1. Introduction

The analysis of the vibration responses for stacked solar arrays exposed to a reverberant acoustic excitation is very important, since the thin and light solar arrays are very sensitive to the acoustic field which could bring about severe damage to the structure. Such analysis is difficult, because the peculiar random acoustic excitation is hard to simulate accurately, and the solar array panels are strongly coupled with the narrow cavities between the panels. The FEM (Finite Element Method)-BEM (Boundary Element Method) method is usually believed to be an effective way to analyze this coupling problem in the low frequency (eg, below 100Hz).

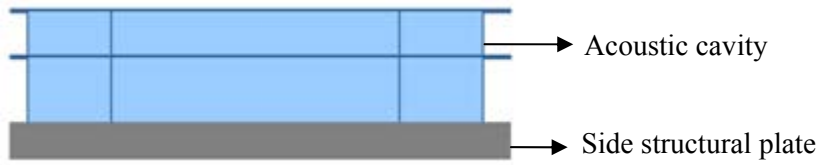


Figure 1: Schematic of the solar array

This paper presents a method to model an acoustic diffuse field by combining uncorrelated plane waves simply, which improves the analysis efficiency greatly for the FEM-BEM approach. And finally, the vibro-acoustic problem for spacecraft solar arrays is simulated using FEM-BEM method and the results are validated by the test data.

2. Basic theory of coupled FEM-BEM

2.1 Equations of coupled FEM-BEM analysis

The coupled FEM-BEM equations are established as follows, if the structural parts are modeled by FEM and the acoustic fields with BEM.

$$\begin{bmatrix} \mathbf{K} + i\omega\mathbf{C} - \omega^2\mathbf{M} & \mathbf{L}_c \\ \mathbf{L}_c^T & \frac{\mathbf{D}}{\rho_0\omega^2} \end{bmatrix} \begin{Bmatrix} \boldsymbol{\mu} \\ \mathbf{q} \end{Bmatrix} = \begin{Bmatrix} \mathbf{F}_s \\ \mathbf{F}_a \end{Bmatrix}, \quad (1)$$

Where, \mathbf{K} 、 \mathbf{C} 、 \mathbf{M} are the structure stiffness、damping and mass matrix respectively; ω is the frequency; \mathbf{L}_c is the coupled matrix; ρ_0 is the air density; \mathbf{D} is the boundary effect matrix; \mathbf{F}_s is the force vector excited on the structure; \mathbf{F}_a is the acoustic vector; $\boldsymbol{\mu}$ is the displacement vector; \mathbf{q} is the pressure jump on the boundary element (Indirect BEM).

Transform equation (1),

$$\begin{aligned} \begin{Bmatrix} \boldsymbol{\mu} \\ \mathbf{q} \end{Bmatrix} &= \begin{bmatrix} \mathbf{K} + i\omega\mathbf{C} - \omega^2\mathbf{M} & \mathbf{L}_c \\ \mathbf{L}_c^T & \frac{\mathbf{D}}{\rho_0\omega^2} \end{bmatrix}^{-1} \begin{Bmatrix} \mathbf{F}_s \\ \mathbf{F}_a \end{Bmatrix} \\ &= \begin{bmatrix} \mathbf{H}_{11} & \mathbf{H}_{12} \\ \mathbf{H}_{21} & \mathbf{H}_{22} \end{bmatrix} \begin{Bmatrix} \mathbf{F}_s \\ \mathbf{F}_a \end{Bmatrix} = [\mathbf{H}] \begin{Bmatrix} \mathbf{F}_s \\ \mathbf{F}_a \end{Bmatrix} \end{aligned} \quad (2)$$

Where \mathbf{H} is the transmission function matrix. If $\{\mathbf{F}_s\}=0$, then

$$\{\boldsymbol{\mu}\} = \mathbf{H}_{12} \times \{\mathbf{F}_a\} \quad (3)$$

Where \mathbf{H}_{12} is the transmission function matrix between the acoustic excitation and the structural vibration response. If the acoustic load are random, then

$$\mathbf{S}_{\mu\mu} = \mathbf{H}_{12} \cdot \mathbf{S}_{AA} \cdot \mathbf{H}_{12}^H \quad (4)$$

Where $\mathbf{S}_{\mu\mu}$ and \mathbf{S}_{AA} are power spectral density of structural displacement response and that of the acoustic load respectively.

2.2 Acoustic diffuse field modeled by combining uncorrelated plane waves linearly

The plane waves are distributed evenly along the longitude and the latitude of a fictitious sphere (corresponding to the 4π solid angle) as shown in Fig.2.

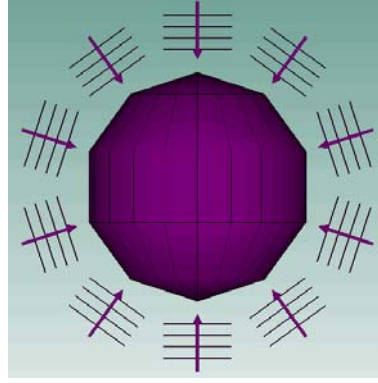


Figure 2: The distribution of plane waves

Suppose $\theta = [\theta_1, \theta_2, \dots, \theta_m]$ in the longitudinal direction, where $\theta_1 = \pi/(2m)$ in the latitudinal direction, $\theta_i = \theta_1 + \pi \times (i-1)/m$, ($i = 2, 3, \dots, m$) and $\psi = [\psi_1, \psi_2, \dots, \psi_n]$, where $\psi_j = 2\pi j/n$, ($j = 1, 2, 3, \dots, n$). Then, totally $m \times n$ uncorrelated plane waves PW_{ij} , with directions represented by $[\theta_i, \psi_j]$ are obtained.

If each plane-wave sound pressure amplitude is symbolized by P_{ij} , and the reverberant sound pressure is P_0 , the following relations should be established.

$$\sum_{i=1}^m \sum_{j=1}^n \frac{(P_{ij})^2}{2} = P_0^2 \quad (5)$$

For each plane wave PW_{ij} , with the direction $[\theta_i, \psi_j]$ and the solid angle $\sin\theta_i \times \Delta\theta \times \Delta\psi$, where $\Delta\theta = \pi/m$, $\Delta\psi = 2\pi/n$, the energy in the solid angle is $P_{ij}^2 / (2 \sin\theta_i \times \Delta\theta \times \Delta\psi)$.

$$\frac{(P_{11})^2}{2 \sin\theta_1 \times \Delta\theta \times \Delta\psi} = \frac{(P_{12})^2}{2 \sin\theta_1 \times \Delta\theta \times \Delta\psi} = \dots = \frac{(P_{mn})^2}{2 \sin\theta_m \times \Delta\theta \times \Delta\psi} \quad (6)$$

From equations (5) and (6), P_{ij} can be derived as follows.

$$P_{ij}^2 = 2 \times \left[\frac{\sin\theta_i}{\left(\sum_{i=1}^m \sin\theta_i \right) \times n} P_0^2 \right] \quad (7)$$

For the plane wave PW_a ($a = 1, 2, \dots, m \times n$), with the direction angle $[\theta_a, \psi_a]$ and the pressure p_a , set the wave number by k and define the three components of k by $k_{a,x} = k \sin\theta_a \times \cos\psi_a$, $k_{a,y} = k \sin\theta_a \times \sin\psi_a$ and $k_{a,z} = k \cos\theta_a$. If there are l nodes on the coupling area, and the coordinates for each node are $[x_u, y_u, z_u]$, ($u = 1, 2, \dots, l$), then the acoustic load matrix for plane waves $\mathbf{P}_{l \times (m \times n)}$ is derived as follows.

$$\mathbf{P}_{l \times (m \times n)} = \begin{bmatrix} \frac{p_1}{\sqrt{2}} e^{-i(k_{1,x} \cdot x_1 + k_{1,y} \cdot y_1 + k_{1,z} \cdot z_1)} & \dots & \frac{p_{m \times n}}{\sqrt{2}} e^{-i(k_{m \times n,x} \cdot x_1 + k_{m \times n,y} \cdot y_1 + k_{m \times n,z} \cdot z_1)} \\ \vdots & \dots & \vdots \\ \frac{p_l}{\sqrt{2}} e^{-i(k_{l,x} \cdot x_l + k_{l,y} \cdot y_l + k_{l,z} \cdot z_l)} & \dots & \frac{p_{m \times n}}{\sqrt{2}} e^{-i(k_{m \times n,x} \cdot x_l + k_{m \times n,y} \cdot y_l + k_{m \times n,z} \cdot z_l)} \end{bmatrix} \quad (8)$$

The auto-spectral density matrix is

$$\mathbf{S}_{AA} \approx \mathbf{P}_{l \times (m \times n)} \cdot \mathbf{I} \cdot \mathbf{P}_{l \times (m \times n)}^H \quad (9)$$

Where \mathbf{S}_{AA} is Hermite matrix, $\mathbf{S}_{AA} \in \mathbb{C}^{l \times l}$; \mathbf{I} is unity.

Now prove \mathbf{S}_{AA} in equation (9) meets the requirement for reverberant sound field.

From equation (5)

$$\mathbf{S}_{AA,uu} = \frac{1}{2} \sum_{a=1}^{m \times n} p_a^2 = p_0^2, \quad (10)$$

$$S_{AA,uv} = \frac{1}{2} \sum_{a=1}^{m \times n} p_a^2 \exp \left\{ i \left[k_{a,x} (x_u - x_v) + k_{a,y} (y_u - y_v) + k_{a,z} (z_u - z_v) \right] \right\}, \quad (u, v = 1, 2, \dots, l), \quad (11)$$

Where $S_{AA,uu}$ 、 $S_{AA,uv}$ are auto-spectral and cross-spectral density between node u and node v respectively.

Simplify equation (11),

$$\begin{aligned} S_{AA,uv} &= \frac{1}{2} \sum_{a=1}^{m \times n} p_a^2 \exp \left\{ i \left[k_{a,x} (x_u - x_v) + k_{a,y} (y_u - y_v) + k_{a,z} (z_u - z_v) \right] \right\} \\ &= \frac{1}{2} \sum_{a=1}^{m \times n} p_a^2 \cos \left[k_{a,x} (x_u - x_v) + k_{a,y} (y_u - y_v) + k_{a,z} (z_u - z_v) \right] + \\ &\quad \frac{1}{2} i \sum_{a=1}^{m \times n} p_a^2 \sin \left[k_{a,x} (x_u - x_v) + k_{a,y} (y_u - y_v) + k_{a,z} (z_u - z_v) \right] \\ &= \frac{1}{2} \sum_{a=1}^{m \times n} p_a^2 \cos(k \cdot r \cdot \cos \beta_a) + \frac{1}{2} i \sum_{a=1}^{m \times n} p_a^2 \sin(k \cdot r \cdot \cos \beta_a) \end{aligned} \quad (12)$$

where

$$\cos \beta_a = \sin \theta_a \cos \psi_a \sin \vartheta \cos \alpha + \sin \theta_a \sin \psi_a \sin \vartheta \sin \alpha + \cos \theta_a \cos \vartheta \quad (13)$$

Then

$$\gamma_{uv} = \frac{S_{AA,uv}}{\sqrt{S_{AA,uu}} \times \sqrt{S_{AA,vv}}} = \frac{\frac{1}{2} \sum_{a=1}^{m \times n} p_a^2 \cos(k \cdot r \cdot \cos \beta_a) + \frac{1}{2} i \sum_{a=1}^{m \times n} p_a^2 \sin(k \cdot r \cdot \cos \beta_a)}{p_0^2} \quad (14)$$

From equations (10) and (14), it can be derived as follows.

$$\begin{aligned} \gamma_{uv} &= \frac{\sum_{a=1}^{m \times n} \frac{\sin \theta_a}{\sum_{a=1}^{m \times n} \sin \theta_a} \times \cos(k \cdot r \cdot \cos \beta_a) + i \sum_{a=1}^{m \times n} \frac{\sin \theta_a}{\sum_{a=1}^{m \times n} \sin \theta_a} \times \sin(k \cdot r \cdot \cos \beta_a)}{\sum_{a=1}^{m \times n} \frac{\sin \theta_a \cdot \Delta \theta \cdot \Delta \psi}{\left(\sum_{a=1}^{m \times n} \sin \theta_a \right) \cdot \Delta \theta \cdot \Delta \psi} \times \cos(k \cdot r \cdot \cos \beta_a) +} \\ &= \frac{\sum_{a=1}^{m \times n} \frac{\sin \theta_a \cdot \Delta \theta \cdot \Delta \psi}{\left(\sum_{a=1}^{m \times n} \sin \theta_a \right) \cdot \Delta \theta \cdot \Delta \psi} \times \cos(k \cdot r \cdot \cos \beta_a) +} \\ &\quad i \sum_{a=1}^{m \times n} \frac{\sin \theta_a \cdot \Delta \theta \cdot \Delta \psi}{\left(\sum_{a=1}^{m \times n} \sin \theta_a \right) \cdot \Delta \theta \cdot \Delta \psi} \times \sin(k \cdot r \cdot \cos \beta_a) \circ \end{aligned} \quad (15)$$

If m and n are infinite numbers, i.e. $\Delta \theta \rightarrow 0$ 、 $\Delta \psi \rightarrow 0$, then

$$\begin{aligned} \lim_{m,n \rightarrow \infty} \sum_{a=1}^{m \times n} \sin \theta_a \cdot \Delta \theta \cdot \Delta \psi \cos(k \cdot r \cdot \cos \beta_a) &\approx \int_0^{2\pi} \int_0^\pi \sin \theta \cos(k \cdot r \cdot \cos \beta) d\theta d\psi = \frac{4\pi \sin(k \cdot r)}{k \cdot r}. \\ \lim_{m,n \rightarrow \infty} \left(\sum_{a=1}^{m \times n} \sin \theta_a \right) \cdot \Delta \theta \cdot \Delta \psi &\approx \int_0^{2\pi} \int_0^\pi \sin \theta d\theta d\psi = 4\pi. \\ \lim_{m,n \rightarrow \infty} \sum_{a=1}^{m \times n} \sin \theta_a \cdot \Delta \theta \cdot \Delta \psi \sin(k \cdot r \cdot \cos \beta_a) &\approx \int_0^{2\pi} \int_0^\pi \sin \theta \sin(k \cdot r \cdot \cos \beta) d\theta d\psi = 0, \end{aligned} \quad (16)$$

Where $\cos \beta = \sin \theta \cos \psi \sin \vartheta \cos \alpha + \sin \theta \sin \psi \sin \vartheta \sin \alpha + \cos \theta \cos \vartheta$. From equation (16) and (15), it can be seen that

$$\gamma_{uv} \approx \frac{\sin(k \cdot r)}{k \cdot r} \circ \quad (17)$$

From equations (9) and (4), the structural responses can be calculated.

$$\begin{cases} \mathbf{S}_{\mu\mu} = \mathbf{H}_{12} \cdot \mathbf{S}_{AA} \cdot \mathbf{H}_{12}^T \approx \mathbf{H}_{12} \cdot \mathbf{P}_{l \times (m \times n)} \cdot \mathbf{I} \cdot \mathbf{P}_{l \times (m \times n)}^H \cdot \mathbf{H}_{12}^H = \mathbf{R} \cdot \mathbf{I} \cdot \mathbf{R}^H \\ \mathbf{R} = \mathbf{H}_{12} \cdot \mathbf{P}_{l \times (m \times n)} \end{cases} \quad (18)$$

Where the a column of the matrix \mathbf{R} symbolizes the load for the plane wave PW_a .

3. Numerical calculation and verifications

3.1 Acoustic diffuse field modeled by combining uncorrelated plane waves linearly

Numerical calculation is realized by MATLAB. Set $m = n = 10$, $r = 0.2$ m, $\vartheta = \pi/3$, $\alpha = \pi/7$, $\omega = 600\pi$, and random phases for each plane wave. Finally, the cross-spectral density $\gamma_{uv} = 0.8108$, and the theoretical one is 0.8073, with error of 0.43%. Set $m=20$, $n=10$, Then $\gamma_{uv} = 0.8082$, and the error is 0.11%. That shows the derivations in this paper is correct, and the analysis results should be better if m and n becomes bigger.

3.2 Comparison of DBEM and IBEM

Comparison of DBEM (Direct Boundary Element Method) and IBEM (Indirect Boundary Element Method) are shown in Fig.3. It can be seen that there is little difference between them so far as the main peak responses are concerned.

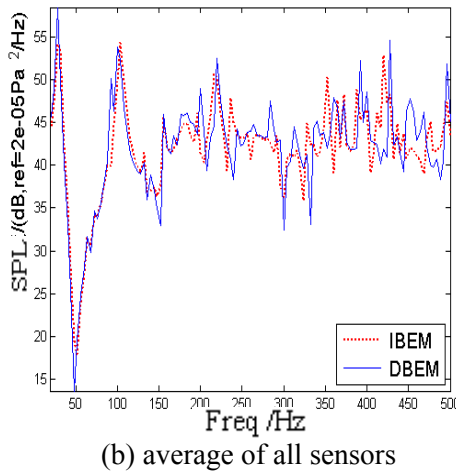
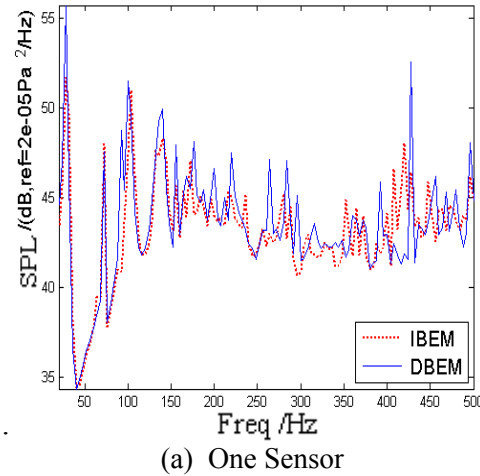


Figure 3: Comparison between the pressure PSD result of DBEM and that of IBEM

3.3 Response analysis and verification

Here we analyze a spacecraft model with solar arrays under diffuse sound excitation. Fig.4 shows the SPL of the diffuse acoustic field.

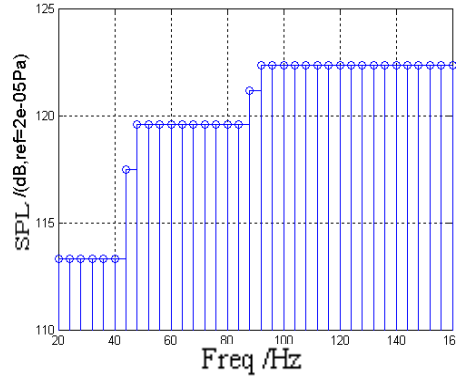


Figure 4: The SPL of the diffuse acoustic field

Three load cases are compared by 4×6 plane waves, 5×10 plane waves and 15×12 plane waves. It can be seen from Fig.5 that 50 plane waves are enough in general for similar analysis.

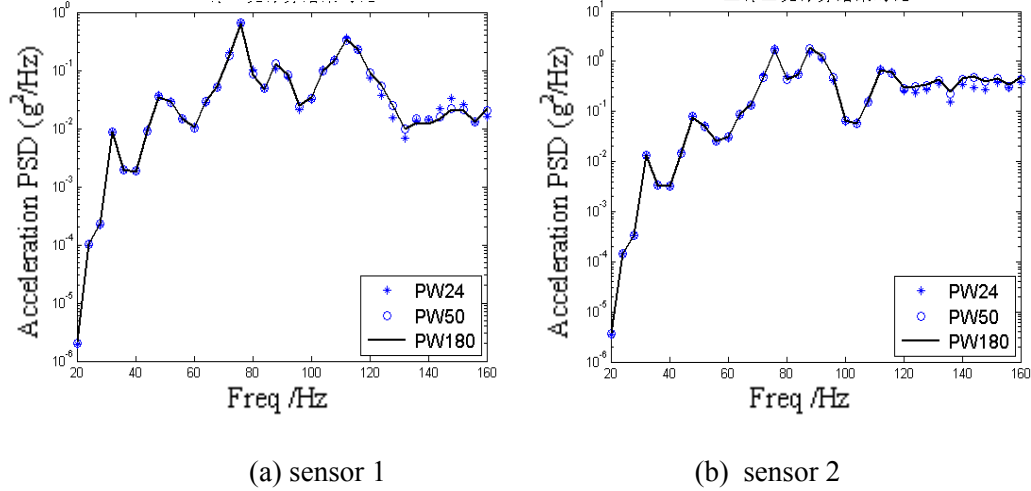


Figure 5: Calculation results comparison of two measurement points in three load cases

It is shown in Fig.6 that there is a notable SPL (Sound Pressure Level) increase in the narrow air gaps between panels if the excitation frequency becomes closer to the narrow cavity resonance modes.

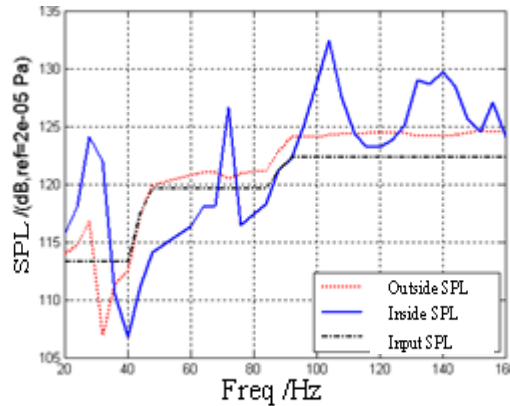


Figure 6: Comparison between the inside and outside pressure

Fig.7 shows the analysis response results compared with the test data on the four acceleration sensors. The errors for 4 sensors are 1.5dB, 2.2dB, -0.7dB and -0.9 dB respectively, which are ac-

ceptable in the engineering view.

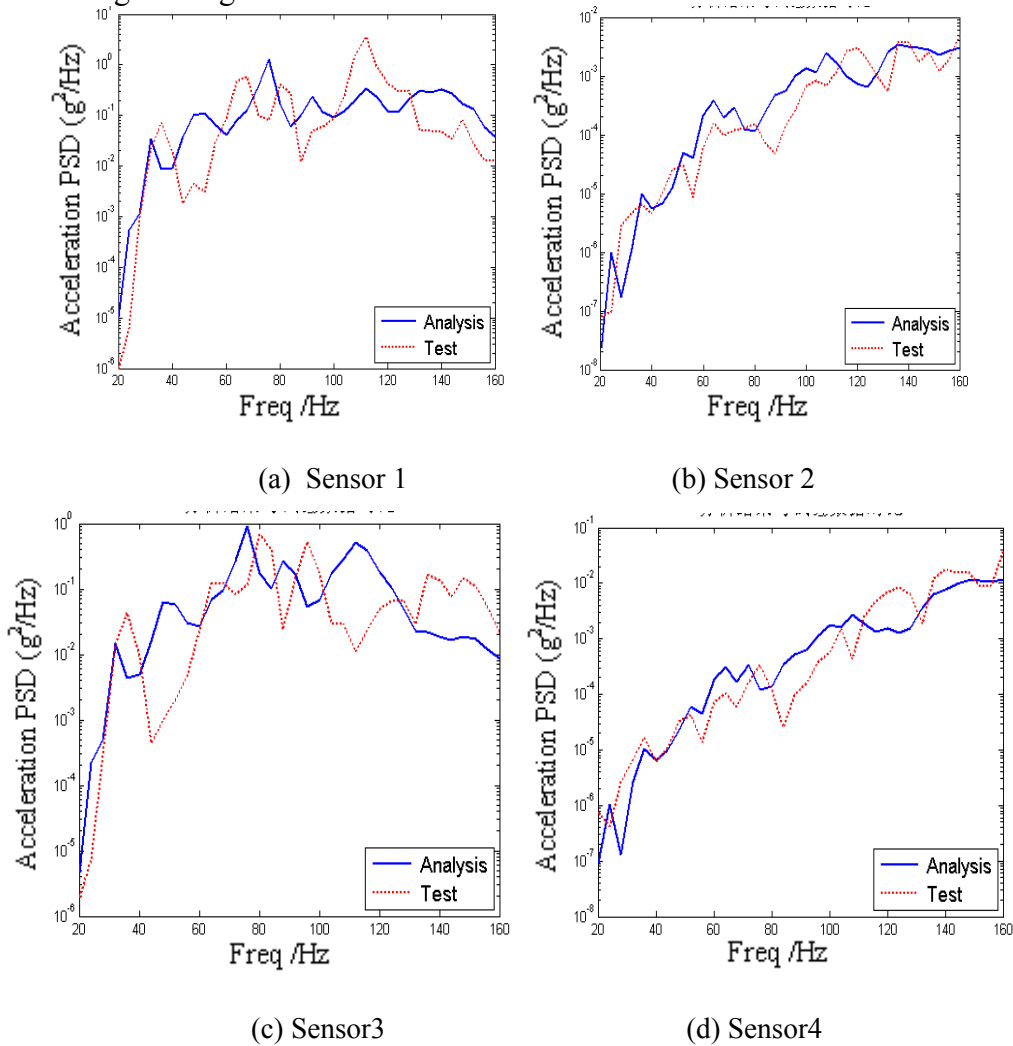


Figure 7: Comparison between the analysis data and test data (load case 2)

4. Conclusions

This paper presents a method to model an acoustic diffuse field by combining uncorrelated plane waves linearly and proves its veracity theoretically. The parameters for each plane wave are also obtained through derivation in the paper. After that, the vibro-acoustic problem for spacecraft solar arrays is simulated using FEM-BEM method and the results are validated by the test data, which shows that the method is theoretically correct and could be used to analyze the vibro-acoustic response of spacecraft. Besides, it is shown that there is a notable SPL (Sound Pressure Level) increase in the narrow air gaps between panels if the excitation frequency becomes closer to the narrow cavity resonance modes and the coupling effects between panels and the air gaps must be considered.

REFERENCES

- 1 Zou Yuanjie, Han Zengrao, Zhang Jin. Research Progress on Full-frequency Prediction Techniques of Spacecraft's Mechanical Environment[J]. Advances in Mechanics ,2012,42(4):445-454
- 2 Norton M P, Karczub D G. Fundamentals of noise and vibration analysis for engineers[M]. 2 ed. Cambridge: Cambridge University Press, 2003: 60-62

- 3 Seybert A F, Wu T W, Li W L. A coupled FEM/BEM for fluid-structure interaction using Ritz vectors and eigenvectors[J]. Journal of Vibration and Acoustics, 1993, 115(2): 152-158
- 4 Vlahopoulos N, Raveendra S T, Vallance C, et al. Numerical implementation and applications of a coupling algorithm for structural-acoustic model with unequal discretization and partially interfacing surfaces[J]. Finite Elements in Analysis and Design, 1999, 32(4): 257-277